EJN fens EUROPEAN JOURNAL OF NEUROSCIENCE

European Journal of Neuroscience, pp. 1–9, 2010 doi:10.1111/j.1460-9568.2010.07495.x

Two highly homologous mouse odorant receptors encoded by tandemly-linked *MOR29A* and *MOR29B* genes respond differently to phenyl ethers

Akio Tsuboi,[1,2,*] Takeshi Imai,[1,3,4,*] Hiroyuki K. Kato,[1] Hideyuki Matsumoto,[5] Kei M. Igarashi,[5] Misao Suzuki,[6] Kensaku Mori[5] and Hitoshi Sakano[1]

[1]Department of Biophysics and Biochemistry, Graduate School of Science, The University of Tokyo, Bunkyo-ku, Tokyo 113-0032, Japan

[2]Laboratory for Molecular Biology of Neural System, Advanced Medical Research Center, Nara Medical University, Kashihara, Nara, Japan

[3]Laboratory for Sensory Circuit Formation, RIKEN Center for Developmental Biology, Kobe, Japan

[4]PRESTO, Japan Science and Technology Agency (JST), Saitama, Japan

[5]Department of Physiology, Graduate School of Medicine, The University of Tokyo, Tokyo, Japan

[6]Center for Animal Resources and Development, Kumamoto University, Kumamoto, Japan

Keywords: calcium imaging, odor response, odorant receptor, optical imaging, transgenic mouse

Abstract

Since the discovery of odorant receptors (ORs) in rodents, most ORs have remained orphan receptors. Even for deorphanized ORs *in vitro*, their *in vivo* properties are largely unknown. Here, we report odor response profiles of two highly homologous mouse ORs, MOR29A and MOR29B, both *in vivo* and *in vitro*. The BAC transgenic mouse was generated, in which olfactory sensory neurons (OSNs) expressing the transgenes *MOR29A* and *MOR29B* were differently tagged with *IRES-gapECFP* and *IRES-gapEYFP*, respectively. *MOR29A*- and *MOR29B*-expressing OSN axons converged on separate but nearby loci on the dorsal surface of the olfactory bulb (OB). Optical imaging of intrinsic signals in the OB identified five different phenyl ethers as candidate ligands for MOR29B. Based on *in vitro* calcium imaging with the isolated OSNs and luciferase assay with heterologous cells, only guaiacol and vanillin were found to be potent agonists for MOR29A and MOR29B. Because of its accessible glomerular locations in the dorsal OB and defined odor response profiles both *in vivo* and *in vitro*, the MOR29A/29B tagging mouse will serve as an excellent tool for studying both odor-signal processing and neural circuitry in the OB.

Introduction

In the mouse main olfactory system, inhaled odorants dissolved in the olfactory mucosa of the olfactory epithelium (OE) are detected with a repertoire of approximately 1000 different odorant receptors (ORs; Buck & Axel, 1991). It is well-established that each olfactory sensory neuron (OSN) expresses only one functional OR gene in a monoallelic manner (Chess *et al.*, 1994; Malnic *et al.*, 1999; Serizawa *et al.*, 2000, 2003). Furthermore, OSN axons expressing a given OR species converge on one of approximately 1000 glomeruli in each mirror map of the right and left olfactory bulb (OB; Ressler *et al.*, 1994; Vassar *et al.*, 1994; Mombaerts *et al.*, 1996). Thus, odorant stimuli that activate a specific set of OSNs in the OE are converted to a topographic map of activated glomeruli in the OB (Mori *et al.*, 2006).

The OB is the first relay station for olfactory signal processing in the brain, where each mitral/tufted (M/T) cell receives inputs from homotypic OSN axons. It is important to study how the odor signals are represented, categorized and processed in the OB. Electrophysiological and imaging studies of the OB revealed a domain organization of the olfactory map – glomeruli for odor ligands with similar functional groups tend to cluster in a particular region of the OB (Mori *et al.*, 2006). At least in the dorsal region of the OB, there appear to be multiple functional domains for distinct innate responses such as fearful, aversive, attractive and social behaviors (Kobayakawa *et al.*, 2007; Matsumoto *et al.*, 2010).

Since the discovery of OR genes, identification of OR ligands has been challenging because ORs are poorly expressed in the heterologous expression system. To date, dozens of ORs have been deorphanized (Saito *et al.*, 2004, 2009); however, odor response profiles *in vivo* do not faithfully mirror those found *in vitro* (Oka *et al.*, 2006; Zhuang & Matsunami, 2007). Although numerous OR genes have been tagged with fluorescent protein genes, odor response profiles *in vivo* have been described only for a few OR species (Mombaerts, 2004).

Correspondence: Akio Tsuboi, Akio Tsuboi, [2]Nara Medical University,
E-mail: atsuboi@naramed-u.ac.jp

Hitoshi Sakano, [1]The University of Tokyo,
E-mail: sakano@mail.ecc.u-tokyo.ac.jp

*These authors contributed equally to this work.

Received 2 June 2010, revised 7 September 2010, accepted 6 October 2010

Our group has been working on the *MOR28* cluster located in the mouse chromosome 14, which includes seven OR genes, *MOR28*, *10*, *83*, *29A*, *29B*, *30A* and *30B* (Tsuboi *et al.*, 1999; Nagawa *et al.*, 2002). Possibly due to gene conversion during evolution, *MOR29A* and *MOR29B* genes have been kept quite similar to each other; their protein products share the 95% amino-acid sequence homology. In order to study the odor receptive range and axonal projection of these highly homologous ORs, we generated a mouse line in which the transgenic *MOR29A* and *MOR29B* were differently tagged with two fluorescent protein genes, enhanced cyan-fluorescent protein (ECFP) and enhanced yellow-fluorescent protein (EYFP), respectively. MOR29A and MOR29B glomeruli were identified in adjacent areas on the dorsal surface of the OB.

In the present study, we have analyzed odor response profiles of MOR29A and MOR29B, both *in vivo* and *in vitro*. It was found that guaiacol and vanillin are potent agonists for MOR29A and MOR29B *in vitro*. These results will help us understand how odor signals are processed and control the neural circuits in the OB.

Materials and methods

Transgenic mice

Our animal research was approved by the Committees for Animal Experimentation in both the University of Tokyo and Nara Medical University, and was conducted in accordance with their guidelines. MOR29A/29B BAC transgenic mice were generated using a C57BL/6 mouse BAC clone (RPCI-23 339P24) as described previously (Nakatani *et al.*, 2003). The internal ribosome entry site (*IRES*)-*gapECFP* and *IRES-gapEYFP* cassettes were introduced just after the stop codons of *MOR29A* and *MOR29B*, respectively. The N-terminal 20-aa sequence of mouse GAP-43 was used as a gap tag (Serizawa *et al.*, 2000).

Fluorescent images

Mice were deeply anesthetized with sodium pentobarbital (2.5 mg/animal) and perfused intracardially with 4% paraformaldehyde. For whole-mount inspections, OBs were dissected from fixed samples and mounted on coverslips. Cryostat sections of 16 μm thickness were collected on glass slides. Fluorescent images of whole-mount OBs and OE sections were photographed with a fluorescence microscope, Model IX70 (Olympus, Tokyo, Japan), equipped with a cooled CCD camera, the ORCA-ER (Hamamatsu Photonics, Hamamatsu, Japan). Acquisition and quantification of digital photos were done with AQUACOSMOS (Hamamatsu Photonics).

Optical imaging of intrinsic signals

Optical and fluorescent imaging was performed on adult male MOR29A/29B transgenic mice ($n = 4$) as described previously (Uchida *et al.*, 2000; Matsumoto *et al.*, 2010). Dorsal views of glomeruli in the OB were constructed and superimposed onto the optical imaging signals using ECFP/EYFP fluorescence signals and blood vessels as references.

Fura-2 calcium imaging of dissociated OSNs

Candidate agonists for MOR29A and MOR29B were first screened by intrinsic signal imaging of the OB. The identified molecules were then analyzed using fura-2 calcium imaging of isolated OSNs as described previously (Imai *et al.*, 2006). Odorants in Ringer's solution were applied for 10 s at 1- to 3-min intervals. Data were acquired with an AQUACOSMOS RATIO imaging system (Hamamatsu Photonics). Fura-2 fluorescence at 510 nm was acquired every 2 s with excitation at 340/380 nm.

Luciferase assays using the Hana2i cell line

Flip-In-293 cells (Invitrogen, Carlsbad, CA, USA) were used to establish a stable cell line, termed Hana2i, expressing RTP1S and Ric8b. Ric8b was bicistronically expressed using a synthetic IRES sequence (Chappell *et al.*, 2000). Hana2i cells were grown in DMEM supplemented with 10% FBS. Hana2i cells in a 96-well format were transfected with 150 ng/well pME18S-F-R-OR, 25 ng/well CRE-Luc2P (pGL4.29[luc2P/CRE/Hygro]; Promega, Madison, WI, USA) and 25 ng/well TK-hRluc (pGL4.74[hRluc/TK]; Promega) using Lipofectamine 2000 (0.5 μL/well; Invitrogen) and incubated for 24 h. The medium was then replaced with DMEM containing odor ligands, and cells were further incubated for 4 h. Luc2P and hRluc activities were differentially quantitated using the Dual-Glo Luciferase assay system (Promega). Luminescence was measured using a TriStar LB941 luminometer (Berthold, Bad Wildbad, Germany). The pME18S-F-R-OR vector contains the *SR*α promoter, N-terminal FLAG and bovine rhodopsin (N-terminal 20 aa) tags, and an OR coding sequence. The complete N-terminal tag sequence is MDYKDDDDKEFMNGTEGPNFYLE. *RTP1S*, *Ric8b* and *OR* coding sequences were PCR-amplified from OE cDNA or genomic DNA from C57BL/6 mice.

Results

OSN axons expressing MOR29A and MOR29B converged on distinct but nearby glomeruli in the dorsal OB

A previous study suggested that gene conversion during evolution has maintained a high homology between the *MOR29A* and *MOR29B* genes (Nagawa *et al.*, 2002). To describe the axonal projection profiles of these closely related OR genes, we generated bacterial artificial chromosome (BAC) transgenic mice. To differently label the two neighboring OR genes, we generated transgenic mice in which *MOR29A* and *MOR29B* genes had been tagged with *IRES-gapECFP* and *IRES-gapEYFP*, respectively, on a BAC clone (Fig. 1A; designated MOR29A/29B). Three BAC transgenic lines were obtained, and one line (no. 1A) was further analyzed because transgenic *MOR29A* and *MOR29B* were expressed in a moderate number of OSNs in this line. The *MOR29A* and *MOR29B* transgenes were expressed in a mutually exclusive manner within the D-zone (zone 1) of the OE (Fig. 1B). Although local permutations have been observed (Strotmann *et al.*, 2000), the axons of differently labeled OSNs converge on nearby loci in the dorsolateral and medial OBs – glomeruli for these two ORs were typically separated by a few to several glomeruli (200 ± 100 μm (mean ± SEM), $n = 11$; Fig. 1C–E).

MOR29B glomeruli respond to five different phenyl ethers

Glomeruli for MOR29A and MOR29B were located on the dorsal OB, where activation patterns for odorants have been extensively studied. We therefore utilized optical imaging of intrinsic signals in the OB (Rubin & Katz, 1999; Uchida *et al.*, 2000; Igarashi & Mori, 2005; Takahashi *et al.*, 2004; Matsumoto *et al.*, 2010) to screen for odor ligands for MOR29A and MOR29B. Two types of fluorescence, ECFP

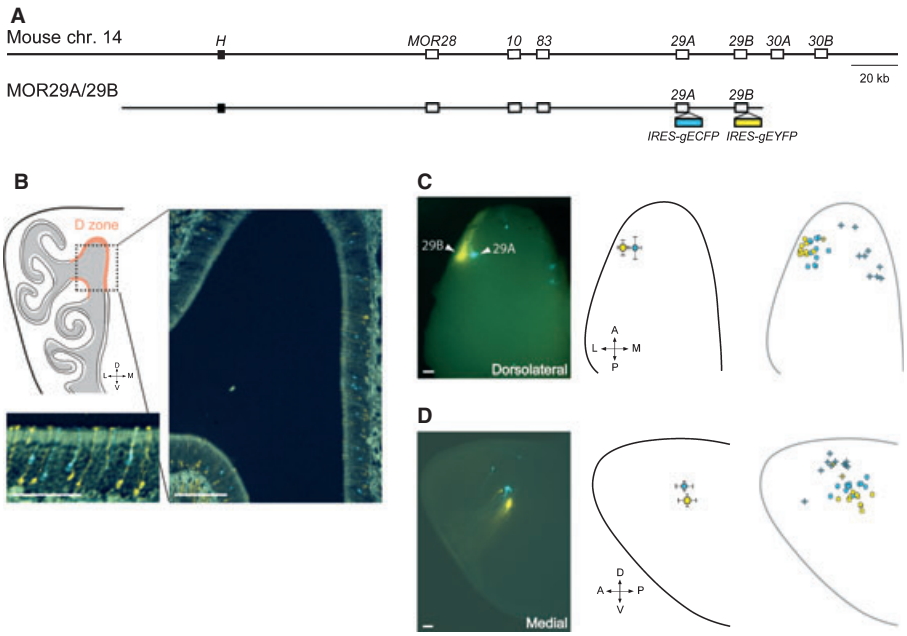

FIG. 1. Generation of MOR29A/29B BAC transgenic mice. (A) Schematic representations of a genomic structure of the *MOR28* cluster and a MOR29A/29B BAC transgenic construct. In a BAC clone containing the *MOR28* cluster (*MOR28-10-83-29A-29B*), *MOR29A* and *MOR29B* genes were tagged with *gapECFP* and *gapEYFP*, respectively, through internal ribosome entry sites (*IRES*). *H*, the locus control region for the *MOR28* cluster; *g*, N-terminal 20-aa sequence from mouse GAP-43, allowing plasma membrane localization. (B) Expression of transgenic *MOR29A* and *MOR29B* in the OE. Schematic representation of the OE section (left panel) shows D-zone (zone 1) in orange. Coronal sections of the OE are shown in photos. The *MOR29A* (cyan) and *MOR29B* (yellow) transgenes were expressed in a mutually exclusive manner within the D-zone of the OE. (C and D) Axonal projection of OSNs expressing *MOR29A* (cyan) and *MOR29B* (yellow). Whole-mount views of (C) the dorsolateral and (D) the medial OBs are shown on the left. The distribution of MOR29A and MOR29B glomeruli (n = 11 for dorsolateral OBs and n = 11 for medial OBs) is schematically illustrated on the right. Major and ectopic glomeruli are indicated by circles and crosses, respectively. The positions of the major glomeruli are summarized in the middle. Bars represent SEM of glomerular positions along anterior–posterior, dorsal–ventral or medial–lateral axes. The axons of differentially labeled OSNs converge on nearby loci (1–3 glomeruli apart) in the D_{II} domain of the dorsal OB (upper panel). A, anterior; P, posterior; L, lateral; M, medial; D, dorsal; V, ventral. Scale bars, 200 μm.

and EYFP, served as references for MOR29A and MOR29B glomeruli (Fig. 2). Intrinsic optical signals (absorption at 705 nm) are thought to reflect presynaptic activity within the glomeruli, i.e. OSN axon termini (Gurden *et al.*, 2006). Aliphatic acids, aliphatic aldehydes, aliphatic alcohols, aliphatic ketones and various other aromatic compounds have been tested in ligand screening because these odorants are known to activate glomeruli in the anterodorsal region of the OB (Uchida *et al.*, 2000; Takahashi *et al.*, 2004; Matsumoto *et al.*, 2010). Some aromatic odorants with phenyl ether groups (Mori *et al.*, 2006), such as guaiacol (> 0.035% changes in n = 8/8 half bulbs), veratrol (n = 6/8), creosol (n = 5/8), vanillin (n = 3/4) and anisole (n = 7/8), specifically and reproducibly changed the intrinsic optical signals in MOR29B glomeruli (Fig. 2; for odorant structure, see Fig. 3). We did not observe any intrinsic signal responses corresponding to MOR29A glomeruli, probably because MOR29A glomeruli were relatively small. These results indicate that the phenyl ethers described above are good candidates for *in vivo* agonists for MOR29B.

OSNs expressing MOR29A and MOR29B responded to guaiacol and vanillin

We then performed fura-2 calcium imaging of isolated OSNs expressing MOR29A and MOR29B using these identified ligands

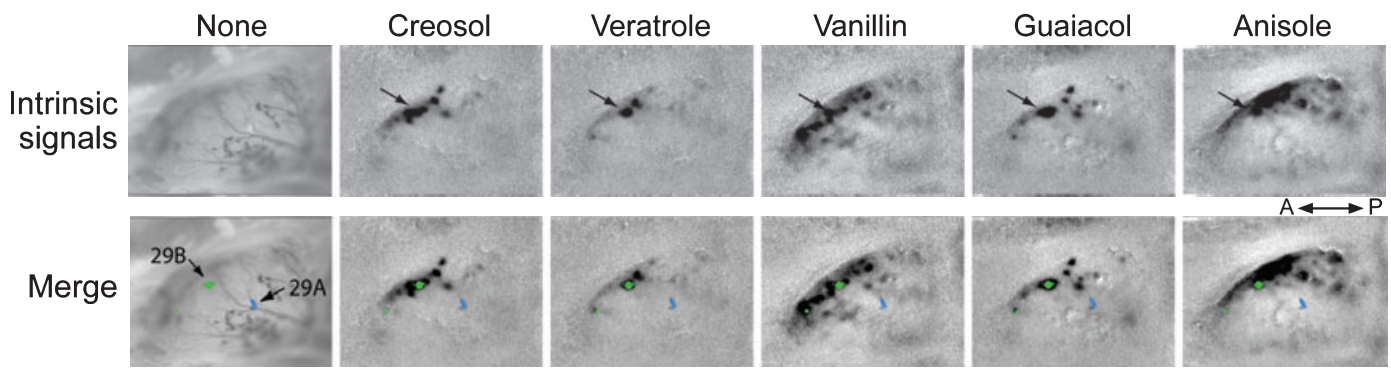

FIG. 2. Optical imaging of intrinsic signals in the OB from MOR29A/29B transgenic mice. The mice were exposed to various odorants, and the dorsal surface of the OB was imaged for intrinsic signals. The images are superimposed with fluorescence images, depicted by blue (MOR29A glomerulus) and green (MOR29B glomerulus) spots. A, anterior; P, posterior.

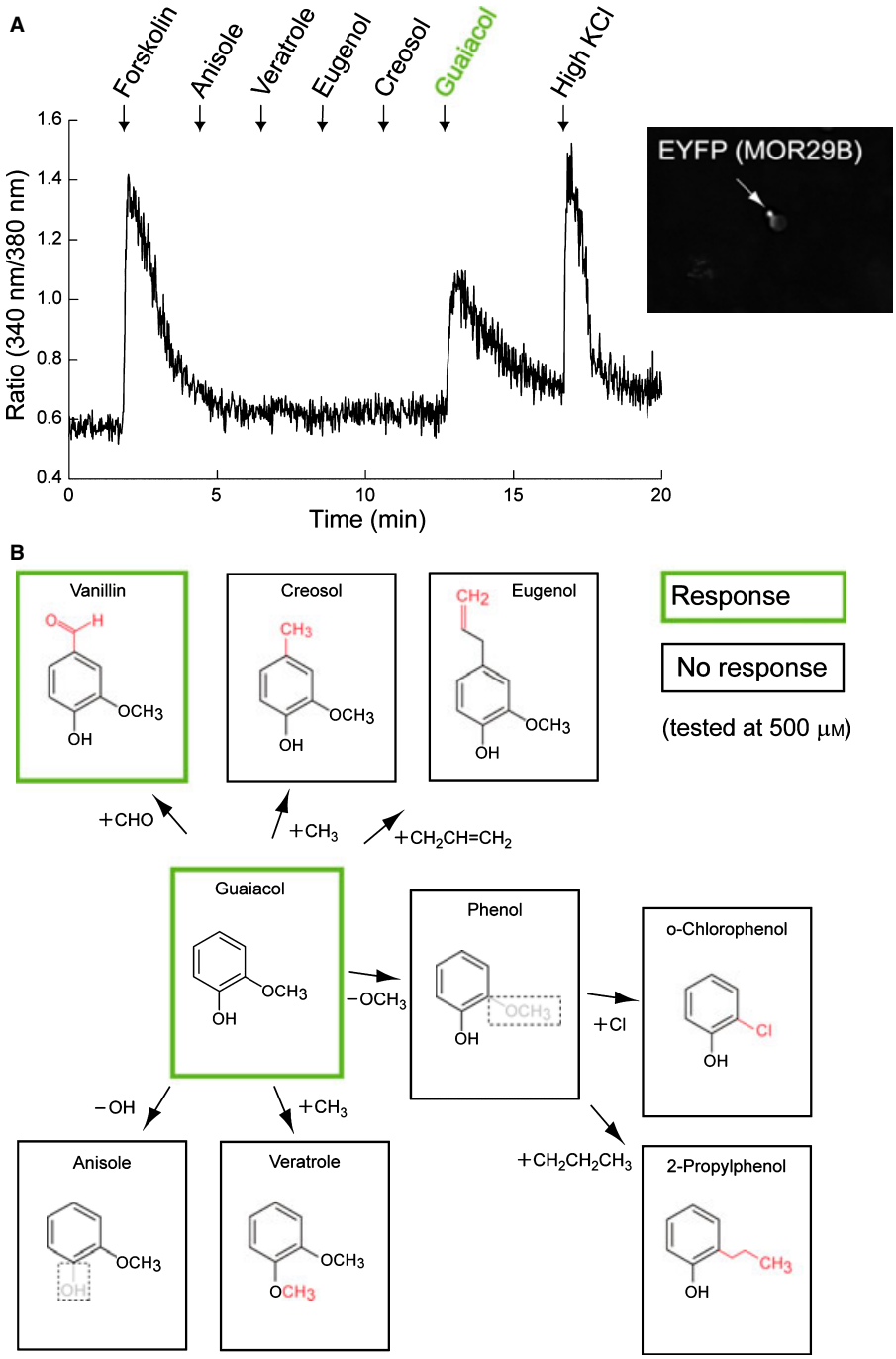

FIG. 3. Molecular receptive range of MOR29B in OSN calcium imaging. (A) As determined by fura-2 calcium imaging, OSNs expressing *MOR29B* specifically responded to 500 μM guaiacol. The inset shows EYFP fluorescence, and an arrow depicts the cell analyzed by calcium imaging. The ratio of fluorescence intensities at 510 nm with excitation at 340/380 nm is shown (left panel). Note that MOR29B OSNs responded to both 50 μM forskolin (an activator of adenylyl cyclase) and high K^+ (100 mM). (B) The molecular receptive range of MOR29B OSNs as determined by calcium imaging experiments. MOR29B OSNs responded to guaiacol and vanillin at concentrations of 500 μM, but not to the other derivatives at this concentration. OSNs responsive to 50 μM forskolin were analyzed. All odorants were tested on at least two OSNs. Responses to guaiacol or vanillin were confirmed at the end of each imaging session.

(Fig. 3). Calcium imaging demonstrated that OSNs expressing MOR29B responded to only guaiacol and vanillin among the candidate molecules tested at 500 μM. Some ligands that appeared to change the intrinsic signals in the OB (i.e. creosol, veratrol and anisole) did not elicit calcium signals in isolated OSNs. MOR29B OSNs were responsive to guaiacol in a dose-dependent manner, with an EC_{50} value of approximately 30 μM (Fig. 4A). MOR29B OSNs also responded to vanillin with a slightly larger EC_{50} value (Figs 3 and 4). Guaiacol and vanillin also activated MOR29A OSNs (Fig. 4B). It should be noted that both MOR29A and MOR29B OSNs responded to forskolin, an activator of adenylyl cyclase, in the control experiments.

Antagonistic odorants have previously been identified for a mouse OR, MOR-EG (Oka *et al.*, 2004). To test the generality of this receptor antagonism, we examined whether chemicals related to guaiacol could suppress the responses of MOR29B OSNs. Increasing concentrations of phenol reversibly inhibited the response to 100 μM

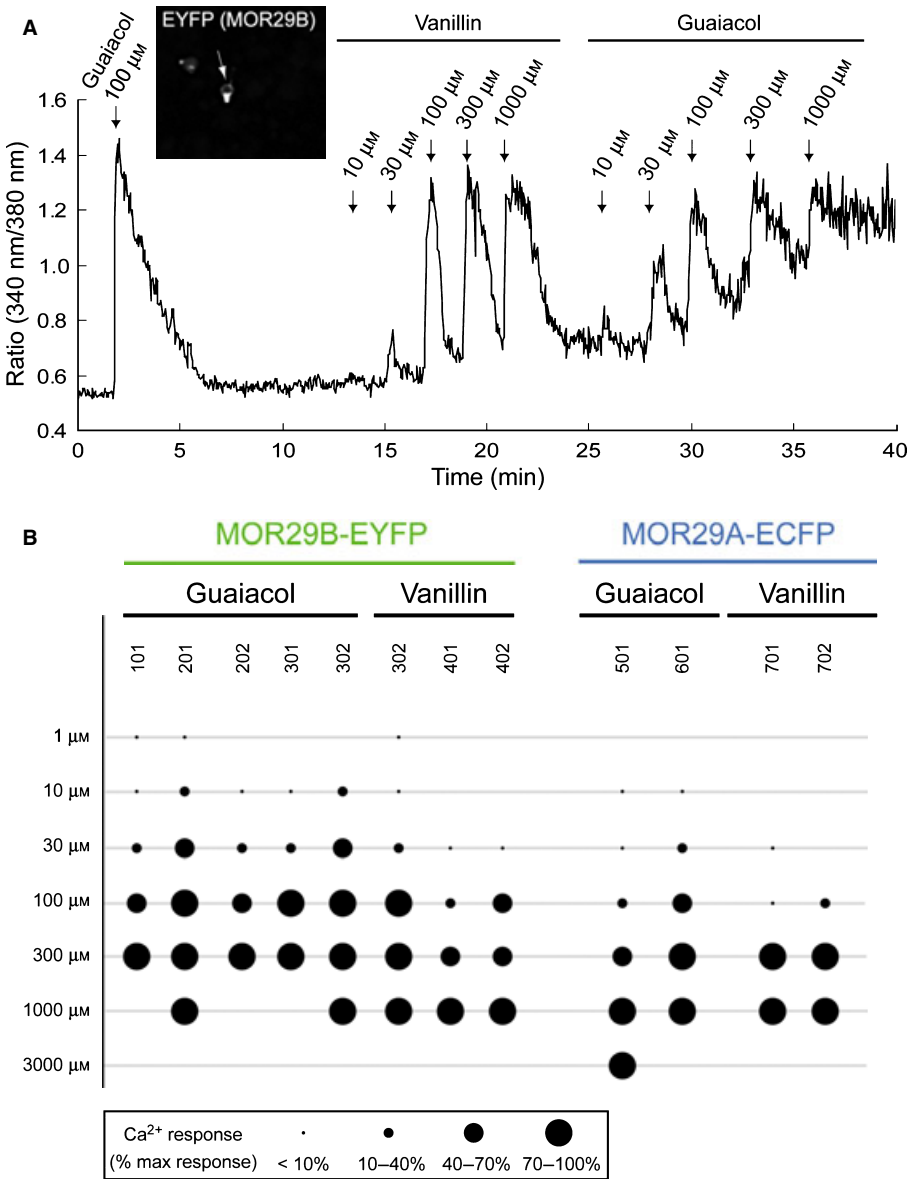

FIG. 4. Dose–response correlation of odor responses in MOR29A and MOR29B OSNs. (A) OSNs expressing *MOR29B* responded to both vanillin and guaiacol in a dose-dependent manner, as determined by fura-2 calcium imaging. An arrow in the inset depicts the cell analyzed by calcium imaging. (B) Dot-plot representation of calcium responses of MOR29A and MOR29B OSNs to guaiacol and vanillin.

guaiacol with an IC_{50} value of approximately 3 mM (Fig. 5). These results indicated that phenol acts as a weak antagonist for MOR29B.

MOR29A and MOR29B were activated by guaiacol and vanillin in a heterologous expression system

We further examined the odor response profiles of MOR29A and MOR29B in a reconstituted system *in vitro*. ORs are poorly expressed in heterologous cells. RTP1S, a chaperone/accessory molecule for ORs, has been reported to dramatically enhance the cell surface expression of ORs in HEK293 cells (Zhuang & Matsunami, 2007). Ric8b, a putative guanine nucleotide exchange factor for Gαolf, has also been reported to augment OR-cAMP signals (Von Dannecker *et al.*, 2006). We therefore generated a HEK293-derived cell line, Hana2i, in which RTP1S and Ric8b are stably expressed from a defined Flp-In locus (Fig. 6A). A rhodopsin N-terminal sequence (rho-tag) was added to ORs to further facilitate cell surface expression. To quantify cAMP signals, we performed a dual luciferase assay: cells were transfected with three expression vectors, cAMP response element – firefly luciferase (CRE-luc2P), thymidine kinase promoter – Renilla luciferase (TK-hRluc), and SRα promoter – OR (SRα-FLAG::rho::OR). When expressed in Hana2i cells, MOR29B exhibited robust responses to guaiacol and vanillin (Fig. 6B). Normalized luciferase activity was increased approximately 100-fold at the maximum, which was a much larger increase than that seen in the other ORs, including MOR29A, MOR-EG, M71, M72 and I7 (data not shown). The EC_{50} value for MOR29B was approximately 30 μM, which was equivalent to that obtained in calcium imaging experiments with the isolated OSNs (Fig. 4B). As in the calcium imaging experiments, vanillin activated MOR29B with a slightly larger EC_{50} value than guaiacol in the Hana2i cells. Similar, albeit smaller,

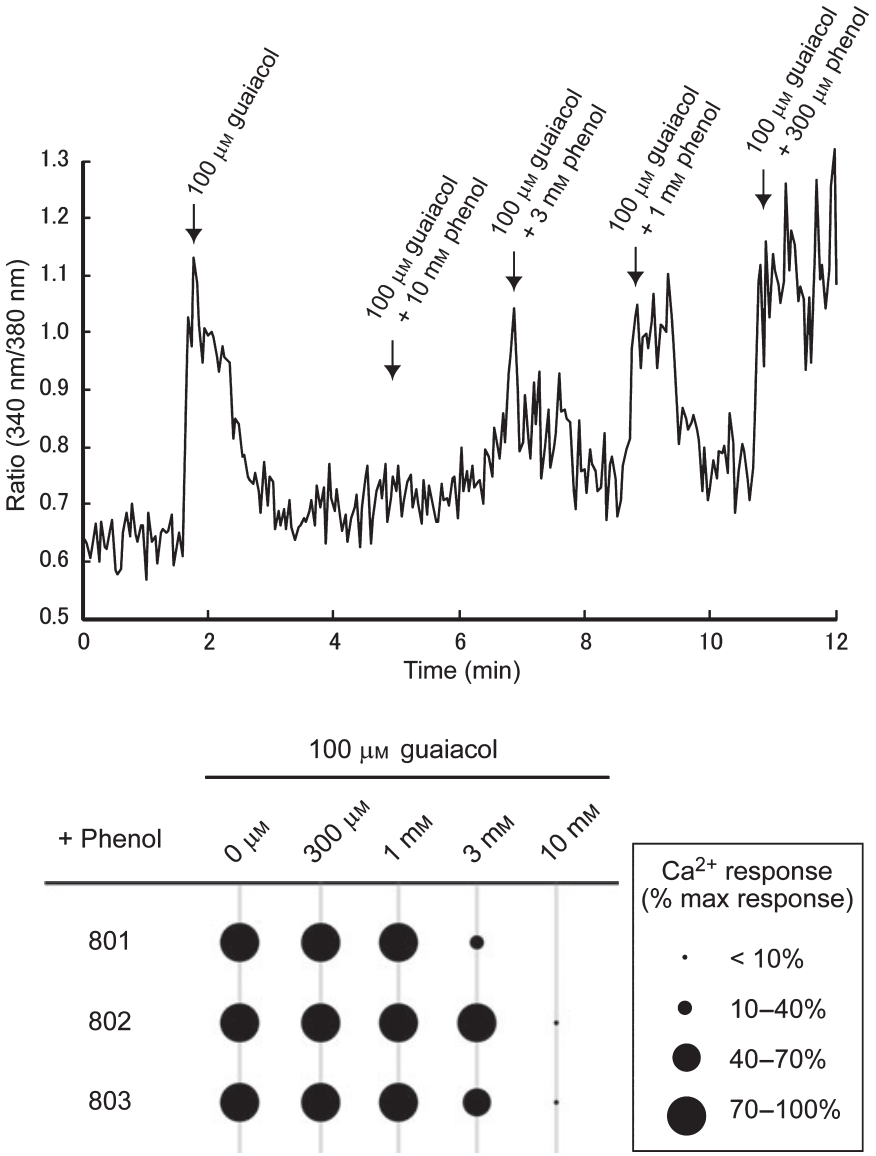

FIG. 5. Phenol antagonizes the guaiacol-induced calcium responses in MOR29B OSNs. In fura-2 calcium imaging experiments, OSNs expressing *MOR29B (EYFP)* responded to 100 μM guaiacol. However, these responses were reversibly inhibited by increasing concentrations of phenol. Responses to guaiacol were completely abolished by 10 mM phenol.

responses were observed with MOR29A (Fig. 6C). These results confirm that guaiacol and vanillin are potent agonists for MOR29A and MOR29B *in vitro*.

Discussion

Molecular receptive range of MOR29B

In the present study, we have generated a BAC transgenic mouse in which the two tandemly linked OR genes, *MOR29A* and *MOR29B*, are differently tagged with *IRES-gapECFP* and *IRES-gapEYFP*, respectively. We attempted to identify odor ligands for these two highly homologous ORs both *in vitro* and *in vivo*. We performed optical imaging of intrinsic signals in the transgenic mouse OB and then screened for odor molecules that activate MOR29A and MOR29B glomeruli. As guaiacol and its related phenyl ethers specifically activated MOR29B glomeruli *in vivo*, we also examined calcium imaging *in vitro* using the isolated OSNs expressing MOR29B. Among various aromatic compounds, only guaiacol and vanillin activated MOR29B-expressing OSNs *in vitro*. It has been reported that MOR-EG responds to vanillin and eugenol but not to guaiacol (Katada *et al.*, 2005). Thus, the molecular receptive range of MOR29B partially overlaps with that of MOR-EG. Previous structure–function studies of MOR-EG indicated that eugenol is recognized by a cavity formed by helices 3, 5 and 6 (Katada *et al.*, 2005). As MOR29B is robustly expressed in HEK293 cells in the presence of chaperone/accessory proteins, it will be interesting to study the structure–function relationships underlying ligand recognition by MOR29B, comparing with those of MOR-EG.

Domain and cluster organization in the OB

Vertebrate OR genes are phylogenetically divided into two distinct classes: class I and class II (Zhang & Firestein, 2002). Class I ORs are expressed exclusively in the D zone of the OE, and OSNs expressing them project their axons to the most anterodorsal area in the OB (D_I domain; Tsuboi *et al.*, 2006). In addition to the class I ORs,

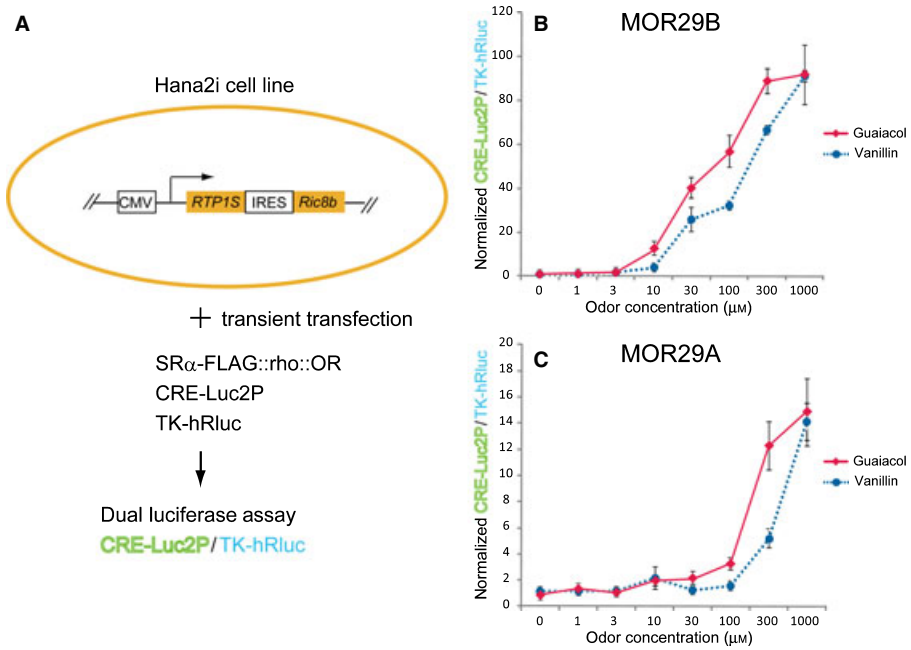

FIG. 6. Luciferase assay in a heterologous cell line, Hana2i. (A) Schematic diagram of the Hana2i cell line and the dual luciferase assay. Expression of Luc2P, under the control of the *CRE* promoter, indicates a level of cAMP signals induced by the odorant-OR interaction. Expression of hRluc is constitutive, driven by the *TK* promoter. (B and C) Luciferase assay of Hana2i cells transfected with either (B) the *MOR29B* or (C) the *MOR29A* expression vector. After transfection, cells were incubated with odorant-containing media for 4 h, and the activities of Luc2P and hRluc were separately measured. The level of Luc2P/hRluc expression in the absence of odorants was defined as 1. Data are expressed as mean ± SEM (n = 3). Results are representative of three independent transfection experiments.

approximately 300 class II ORs are also expressed in the D zone of the OE, but their corresponding glomeruli reside on the periphery of the class I area in the OB (D_{II} domain). The remaining class II ORs are expressed in the V zone of the OE, and their glomerili are found in the ventrolateral area in the OB (V domain; Kobayakawa *et al.*, 2007; Bozza *et al.*, 2009; Matsumoto *et al.*, 2010). The OB is also divided into distinct subdomains at clusters on the basis of the chemical natures and structural features of odor ligands (Mori *et al.*, 2006).

We and others have previously reported that OSNs expressing similar OR genes tend to project their axons to closely proximal areas in the OB (Tsuboi *et al.*, 1999; Strotmann *et al.*, 2000; Feinstein & Mombaerts, 2004). This phenomenon is probably due to the tendency of homologous ORs to generate close levels of cAMP signals, and thereby produce axon guidance molecules (e.g. Neuropilin-1) at similar levels (Imai *et al.*, 2006, 2009). In the present study, we found that two homologous ORs, MOR29A and MOR29B, are both activated by guaiacol and vanillin, as determined by calcium imaging. These results suggest that both MOR29A and MOR29B glomeruli belong to 'Cluster C', which commonly responds to odorants with phenyl-ether groups (Mori *et al.*, 2006). We also found that other homologous mouse ORs, M71 and M72, are activated by acetophenone in Hana2i cells (data not shown). A tendency for homologous ORs to recognize similar odorants, and at the same time to direct OSN axons to similar areas in the OB, may be an additional mechanism underlying the generation of odor domains and clusters in the OB. This idea is also supported by a previous study of eugenol-responsive ORs *in vivo* (Oka *et al.*, 2006).

Possible factors affecting in vitro *vs.* in vivo *response profiles*

Although guaiacol and vanillin elicited robust responses in both MOR29B glomeruli and MOR29B OSN soma (Figs 2 and 4), some ligands that activated MOR29B glomeruli did not activate MOR29B OSNs based on calcium imaging of the isolated OSNs. Furthermore, guaiacol and vanillin were potent agonists of MOR29A and MOR29B as determined by OSN calcium imaging (Fig. 4), while they did not induce significant responses in MOR29A glomeruli (Fig. 2). Because some of these discrepancies may be related to technical issues, for example poor spatial and focal resolution in OB imaging, we cannot exclude the possibility that dim signals are originating in neighboring glomeruli. In contrast to our results with MOR29B, Oka *et al.* (2006) reported that MOR-EG responded to more odorants *in vitro*.

Several factors could underlie the discrepancies in the *in vivo* and *in vitro* odor responses of MOR29A and MOR29B. First, differences in vapor pressure could affect *in vivo* sensitivity – some odorants are efficiently delivered to the nostril by airflow whereas others are not. Second, the solubility of odorants in olfactory mucosal fluid could also affect *in vivo* sensitivity. As equilibrium constants should vary depending on chemical species, predissolved molecules and solvents, odorant concentrations in the odor source or in the air phase cannot easily predict the final odorant concentrations in olfactory mucosal fluid. As a result, for some odorants, saturation concentrations in mucosal fluid may exceed those in saline solution. Furthermore, odorant binding proteins and metabolic enzymes in the mucosa may also account for these differences (Xu *et al.*, 2005; Oka *et al.*, 2006). Third, antagonistic molecules in the olfactory mucosal fluid may also affect *in vivo* responses (Oka *et al.*, 2004); in our OSN calcium imaging experiments, responses of *MOR29B*-expressing OSNs to guaiacol were suppressed by increasing concentrations of phenol (Fig. 5). Finally, inhibitory glomerular neuronal circuits via periglomerular cells in the OB may presynaptically suppress the activity of OSN axon termini (Aroniadou-Anderjaska *et al.*, 2000; McGann *et al.*, 2005; Murphy *et al.*, 2005; Vucinić *et al.*, 2006). The lack of responses in MOR29A glomeruli may be partly due to such circuit-

level inhibition. It will be interesting to quantitatively investigate these phenomena in future studies.

A transgenic tool for the study of OB neural circuitry

In the present study, we have identified the odor ligands for MOR29B both *in vivo* and *in vitro*, i.e. using optical imaging of intrinsic signals, OSN calcium imaging and a Hana2i cell luciferase assay. Although several odor–OR pairs have been established in transgenic mice (e.g. I7 → M71, M71, MOR-EG, MOR23), MOR29B and its ligands are particularly useful for the study of olfactory circuitry for several reasons (Bozza *et al.*, 2002; Oka *et al.*, 2006; Grosmaitre *et al.*, 2006). First, MOR29B glomeruli are located on the dorsal surface of the OB and are easily accessible for optical imaging and electrophysiological experiments. Second, guaiacol and vanillin elicit robust and specific responses in MOR29B glomeruli. Third, in contrast to the rI7 → M71 knockin mouse using the rat OR gene (Bozza *et al.*, 2002), the transgenic MOR29B appears to recapitulate the endogenous one. Fourth, MOR29B is efficiently expressed in heterologous cells in the presence of chaperone/accessory proteins, allowing in-depth studies of ligand–receptor interactions. The MOR29A/29B transgenic mouse described in this study permits the odor-evoked activation of a defined glomerulus in accessible locations and, thus, would serve as an excellent tool for electrophysiological and developmental studies of OB neural circuitry. Our next step is to understand how the odor information is processed in the OB and how the odor-derived signals control the OSN projection and circuit plasticity. Are second-ordered neurons, M/T cells, naïve with respect to projections? Are M/T cells instructed by OSNs? What mediates the synapse formation between the OSN axons and primary dendrite of M/T cell? These interesting questions are to be answered in the future. The transgenic MOR29A/29B system will serve as an excellent model system for studying the axon wiring and neural-circuit formation in the OB.

Acknowledgements

This work was supported by the Specially Promoted Research Grant to H.S. and Grants-in-Aid, Scientific Research for Basic Research (C) and Priority Areas (Cell Sensor) to A.T. from the Ministry of Education, Culture, Sports, Science and Technology, Japan. A.T. was supported by grants from Novartis Foundation, Terumo Foundation, Naito Foundation, Japan Foundation for Applied Enzymology, Urakami Foundation and Daiwa Housing Group (Indoor Environmental Medicine). T.I. was supported by grants from Japan Foundation for Applied Enzymology, Nakajima Foundation and Sumitomo Foundation.

Abbreviations

BAC, bacterial artificial chromosome; ECFP, enhanced cyan-fluorescent protein; EYFP, enhanced yellow-fluorescent protein; IRES, internal ribosome entry site; M/T, mitral/tufted; OB, olfactory bulb; OE, olfactory epithelium; OR, odorant receptor; OSN, olfactory sensory neuron.

References

Aroniadou-Anderjaska, V., Zhou, F.M., Priest, C.A., Ennis, M. & Shipley, M.T. (2000) Tonic and synaptically evoked presynaptic inhibition of sensory input to the rat olfactory bulb via GABA(B) heteroreceptors. *J. Neurophysiol.*, **84**, 1194–1203.

Bozza, T., Feinstein, P., Zheng, C. & Mombaerts, P. (2002) Odorant receptor expression defines functional units in the mouse olfactory system. *J. Neurosci.*, **22**, 3033–3043.

Bozza, T., Vassalli, A., Fuss, S., Zhang, J.J., Weiland, B., Pacifico, R., Feinstein, P. & Mombaerts, P. (2009) Mapping of class I and class II odorant receptors to glomerular domains by two distinct types of olfactory sensory neurons in the mouse. *Neuron*, **29**, 220–233.

Buck, L. & Axel, R. (1991) A novel multigene family may encode odorant receptors: a molecular basis for odorant recognition. *Cell*, **65**, 175–187.

Chappell, S.A., Edelman, G.M. & Mauro, V.P. (2000) A 9-nt segment of a cellular mRNA can function as an internal ribosome entry site (IRES) and when present in linked multiple copies greatly enhances IRES activity. *Proc. Natl. Acad. Sci. USA*, **97**, 1536–1541.

Chess, A., Simon, I., Ceder, H. & Axel, R. (1994) Allelic inactivation regulates olfactory receptor gene expression. *Cell*, **78**, 823–834.

Feinstein, P. & Mombaerts, P. (2004) A contextual model for axonal sorting into glomeruli in the mouse olfactory system. *Cell*, **117**, 817–831.

Grosmaitre, X., Vassalli, A., Mombaerts, P., Shepherd, G.M. & Ma, M. (2006) Odorant responses of olfactory sensory neurons expressing the odorant receptor MOR23: a patch clamp analysis in gene-targeted mice. *Proc. Natl. Acad. Sci. USA*, **103**, 1970–1975.

Gurden, H., Uchida, N. & Mainen, Z.F. (2006) Sensory-evoked intrinsic optical signals in the olfactory bulb are coupled to glutamate release and uptake. *Neuron*, **52**, 335–345.

Igarashi, K.M. & Mori, K. (2005) Spatial representation of hydrocarbon odorants in the ventrolateral zones of the rat olfactory bulb. *J. Neurophysiol.*, **93**, 1007–1019.

Imai, T., Suzuki, M. & Sakano, H. (2006) Odorant receptor-derived cAMP signals direct axonal targeting. *Science*, **314**, 657–661.

Imai, T., Yamazaki, T., Kobayakawa, R., Kobayakawa, K., Abe, T., Suzuki, M. & Sakano, H. (2009) Pre-target axon sorting establishes the neural map topography. *Science*, **31**, 585–590.

Katada, S., Hirokawa, T., Oka, Y., Suwa, M. & Touhara, K. (2005) Structural basis for a broad but selective ligand spectrum of a mouse olfactory receptor: mapping the odorant-binding site. *J. Neurosci.*, **25**, 1806–1815.

Kobayakawa, K., Kobayakawa, R., Matsumoto, H., Oka, Y., Imai, T., Ikawa, M., Okabe, M., Ikeda, T., Itohara, S., Kikusui, T., Mori, K. & Sakano, H. (2007) Innate versus learned odour processing in the mouse olfactory bulb. *Nature*, **450**, 503–508.

Malnic, B., Hirono, J., Sato, T. & Buck, L.B. (1999) Combinatorial receptor codes for odors. *Cell*, **5**, 713–723.

Matsumoto, H., Kobayakawa, K., Kobayakawa, R., Tashiro, T., Mori, K., Sakano, H. & Mori, K. (2010) Spatial arrangement of glomerular molecular-feature clusters in the odorant-receptor-class domains of the mouse olfactory bulb. *J. Neurophysiol.*, **103**, 3490–3500.

McGann, J.P., Pírez, N., Gainey, M.A., Muratore, C., Elias, A.S. & Wachowiak, M. (2005) Odorant representations are modulated by intra- but not interglomerular presynaptic inhibition of olfactory sensory neurons. *Neuron*, **48**, 1039–1053.

Mombaerts, P. (2004) Genes and ligands for odorant, vomeronasal and taste receptors. *Nat. Rev. Neurosci.*, **5**, 263–278.

Mombaerts, P., Wang, F., Dulac, C., Chao, S.K., Nemes, A., Mendelsohn, M., Edmondson, J. & Axel, R. (1996) Visualizing an olfactory sensory map. *Cell*, **79**, 1245–1255.

Mori, K., Takahashi, Y.K., Igarashi, K.M. & Yamaguchi, M. (2006) Maps of odorant molecular features in the Mammalian olfactory bulb. *Physiol. Rev.*, **86**, 409–433.

Murphy, G.J., Darcy, D.P. & Isaacson, J.S. (2005) Intraglomerular inhibition: signaling mechanisms of an olfactory microcircuit. *Nat. Neurosci.*, **8**, 354–364.

Nagawa, F., Yoshihara, S., Tsuboi, A., Serizawa, S., Itoh, K. & Sakano, H. (2002) Genomic analysis of the murine odorant receptor *MOR28* cluster: a possible role of gene conversion in maintaining the olfactory map. *Gene*, **292**, 73–80.

Nakatani, H., Serizawa, S., Nakajima, M., Imai, T. & Sakano, H. (2003) Developmental elimination of ectopic projection sites for the transgenic OR genes that lost zone specificity in the olfactory epithelium. *Eur. J. Neurosci.*, **18**, 2425–2432.

Oka, Y., Nakamura, A., Watanabe, H. & Touhara, K. (2004) An odorant derivative as an antagonist for an olfactory receptor. *Chem. Senses*, **29**, 815–822.

Oka, Y., Katada, S., Omura, M., Suwa, M., Yoshihara, Y. & Touhara, K. (2006) Odorant receptor map in the mouse olfactory bulb: in vivo sensitivity and specificity of receptor-defined glomeruli. *Neuron*, **52**, 857–869.

Ressler, K.J., Sullivan, S.L. & Buck, L.B. (1994) Information coding in the olfactory system: evidence for a stereotyped and highly organized epitope map in the olfactory bulb. *Cell*, **79**, 1245–1255.

Rubin, B.D. & Katz, L.C. (1999) Optical imaging of odorant representations in the mammalian olfactory bulb. *Neuron*, **23**, 499–591.

Saito, H., Kubota, M., Roberts, R.W., Chi, Q. & Matsunami, H. (2004) RTP family members induce functional expression of mammalian odorant receptors. *Cell*, **119**, 679–691.

Saito, H., Chi, Q., Zhuang, H., Matsunami, H. & Mainland, J.D. (2009) Odor coding by a mammalian receptor repertoire. *Sci. Signal.*, **2**, ra9.

Serizawa, S., Ishii, T., Nakatani, H., Tsuboi, A., Nagawa, F., Asano, M., Sudo, K., Sakagami, J., Sakano, H., Ijiri, T., Matsuda, Y., Suzuki, M., Yamamori, T., Iwakura, Y. & Sakano, H. (2000) Mutually exclusive expression of odorant receptor transgenes. *Nat. Neurosci.*, **3**, 687–693.

Serizawa, S., Miyamichi, K., Nakatani, H., Suzuki, M., Saito, M., Yoshihara, Y. & Sakano, H. (2003) Negative feedback regulation ensures the one receptor-one olfactory neuron rule in mouse. *Science*, **302**, 2088–2094.

Strotmann, J., Conzelmann, S., Beck, A., Feinstein, P., Breer, H. & Mombaerts, P. (2000) Local permutations in the glomerular array of the mouse olfactory bulb. *J. Neurosci.*, **20**, 6927–6938.

Takahashi, Y.K., Kurosaki, M., Hirono, S. & Mori, K. (2004) Topographic representation of odorant molecular features in rat olfactory bulb. *J. Neurophysiol.*, **92**, 2413–2427.

Tsuboi, A., Yoshihara, S., Yamazaki, N., Kasai, H., Asai-Tsuboi, H., Komatsu, M., Serizawa, S., Ishii, T., Matsuda, Y., Nagawa, F. & Sakano, H. (1999) Olfactory neurons expressing closely linked and homologous odorant receptor genes tend to project their axons to neighboring glomeruli on the olfactory bulb. *J. Neurosci.*, **19**, 8409–8418.

Tsuboi, A., Miyazaki, T., Imai, T. & Sakano, H. (2006) Olfactory sensory neurons expressing class I odorant receptors converge their axons on an antero-dorsal domain of the olfactory bulb in the mouse. *Eur. J. Neurosci.*, **23**, 1436–1444.

Uchida, N., Takahashi, Y.K., Tanifuji, M. & Mori, K. (2000) Odor maps in the mammalian olfactory bulb: domain organization and odorant structural features. *Nat. Neurosci.*, **3**, 1035–1043.

Vassar, R., Chao, S.K., Sitchera, R., Nunez, J.M., Vosshall, L.B. & Axel, R. (1994) Topographic organization of sensory projections to the olfactory bulb. *Cell*, **79**, 981–991.

Von Dannecker, L.E., Mercadante, A.F. & Malnic, B. (2006) Ric-8B promotes functional expression of odorant receptors. *Proc. Natl. Acad. Sci. USA*, **103**, 9310–9314.

Vucinić, D., Cohen, L.B. & Kosmidis, E.K. (2006) Interglomerular center-surround inhibition shapes odorant-evoked input to the mouse olfactory bulb *in vivo*. *J. Neurophysiol.*, **95**, 1881–1887.

Xu, P., Atkinson, R., Jones, D.N. & Smith, D.P. (2005) Drosophila OBP LUSH is required for activity of pheromone-sensitive neurons. *Neuron*, **45**, 193–200.

Zhang, X. & Firestein, S. (2002) The olfactory receptor gene superfamily of the mouse. *Nat. Neurosci.*, **5**, 124–133.

Zhuang, H. & Matsunami, H. (2007) Synergism of accessory factors in functional expression of mammalian odorant receptors. *J. Biol. Chem.*, **282**, 15284–15293.